引用格式：GAO Minge，YUAN He，XU Min，et al. Research on Feature Extraction of Laser Interference Fringe and Centering Measurement Technology[J]. Acta Photonica Sinica，2022，51(2)：0212002
高铭锣，袁鹤，徐敏，等 . 激光干涉条纹特征提取及定中测量技术研究[J]. 光子学报，2022，51(2)：0212002

激光干涉条纹特征提取及定中测量技术研究

高铭锣[1]，袁鹤[2,3]，徐敏[2,3]，王军华[3,4]，崔海龙[5]
（1 复旦大学 工程与应用技术研究院，上海 200433）
（2 复旦大学 信息科学与工程学院，上海 200438）
（3 上海超精密光学制造工程技术研究中心，上海 200438）
（4 复旦大学 光电研究院，上海 200438）
（5 中国工程物理研究院机械制造工艺研究所，四川 绵阳 621000）

摘　要：针对不透明非球面壳体翻转法测量厚度时，被测件翻转前后需要严格控制定中精度的问题，提出一种基于激光干涉的非接触定中测量技术。配合高精度中空气浮转台、调心调平机构，设计并搭建了一套双向激光干涉定中装置，分别采集翻转前后内外表面不同运动姿态的干涉图，并实时分析其动态特征。基于现代光电探测技术，提出对激光干涉条纹进行实时特征提取算法处理，大幅提高了激光干涉条纹的动态识别精度。对定中精度进行理论分析，并在实验中与确定精度的电感测微计比对验证，实验与理论结果一致，证明所提干涉定中装置及实时特征提取算法可以有效提高定中精度，其绝对误差可达 0.424 μm。使用所提干涉定中装置和特征提取算法成功测量了不透明非球面壳体翻转前后相对于气浮转台旋转轴的定中偏差，满足定中要求，为翻转法厚度测量精度提供了定位保障，提高了轮廓及厚度测量数据的准确性。

关键词：干涉测量；特征提取；动态特征；实时分析；厚度测量
中图分类号：O436.1　　**文献标识码**：A　　**doi**：10.3788/gzxb20225102.0212002

0　引言

不透明非球面壳体广泛应用于航空航天、军事及通讯等领域[1-3]，其壁厚的高精度测量与可靠表征是保障此类构件制造质量和性能可靠性的关键。由于无法直接对其壁厚进行微米级无损检测与评估，通常使用翻转法测量壳体内外轮廓值，然后通过模态分析求解厚度[4-5]。其中，翻转前后的定中测量技术是厚度测量可靠表征的关键。

HEINISCH J等[6]使用两个自准直仪分别测量被测件上下表面的偏心，从而得到定中偏差，其精度可达亚微米。但由于这种方法需要配合特定的物镜进行对焦，且物镜的反复拆装会引入不确定的装配误差，不适用于对翻转前后的非球面壳体进行定中监控和测量。MA Zhen等[7]利用干涉仪完成了非球面反射镜的定中，理论推导了干涉图彗差与定中偏差的关系式，基于彗差来表征定中偏差，从而实现定中测量。但这种间接定中的方法只适用仅含有彗差的干涉图，应用场景局限且精度较低。LANGEHANENBERG P等[8]提出了一种将自准直仪与短相干干涉仪相结合的方法，完成了一组透镜的相对位置和厚度测量，但该方法无法实现不透明非球面壳体的定中测量。FANG Chao等[9]提出了一种成像与干涉相结合的定中方法，其将准直成像光路和干涉光路合二为一，适用于多种定中需求，但该方法采用的光路结构复杂，且要求被测件曲率中心与激光汇聚点重合，因此该方法不适用于对壳体翻转前后进行定中。

基金项目：科学挑战计划（No.JDZZ2016006-01），国家重点研发计划（No. 2020YFB2007600）
第一作者：高铭锣（1997—），女，博士研究生，主要研究方向为光学设计与制造。Email: 19110860002@fudan.edu.cn
导师（通讯作者）：徐敏（1959—），男，研究员，博士，主要研究方向为光学设计、先进光学制造与光电测量等。Email: minx@fudan.edu.cn
收稿日期：2021-06-10；**录用日期**：2021-08-31

为解决不透明非球面壳体厚度测量翻转前后中心难监测的问题，提出了一种新的双向激光干涉定中测量技术。该技术的核心是设计了一套激光干涉仪，辅助现代光电探测技术和干涉条纹特征提取算法，实现了不透明非球面壳体翻转前后高精度定中测量。并通过实验比对验证了该技术的定中精度，证明了所提方法的有效性，提高了非球面壳体厚度测量精度。

1 测量原理

使用激光干涉仪对不透明非球面壳体翻转过程进行定中测量[10]，光路示意如图1。采用开普勒望远系统实现激光束的扩束和准直，激光器出射的光经透镜1汇聚，由针孔滤除边缘杂光达到均匀光强的目的，后经透镜2准直。准直后的光束通过分光棱镜后到达45°反射镜，改变光束方向至垂直于被测件。光束经过透镜组整形后，一部分光从透镜组中的参考球面镜原路返回作为参考光，另一部分光汇聚于非球面壳体的最佳拟合球心处，经被测件反射后作为测量光返回。参考光和测量光在经过分光棱镜和透镜3后在探测器前形成干涉，干涉图由探测器记录。被测件上方安装了相同的激光干涉仪和辅助汇聚透镜，构成双向激光干涉定中测量，能够对被测件翻转前后进行一致性和倾斜监测。

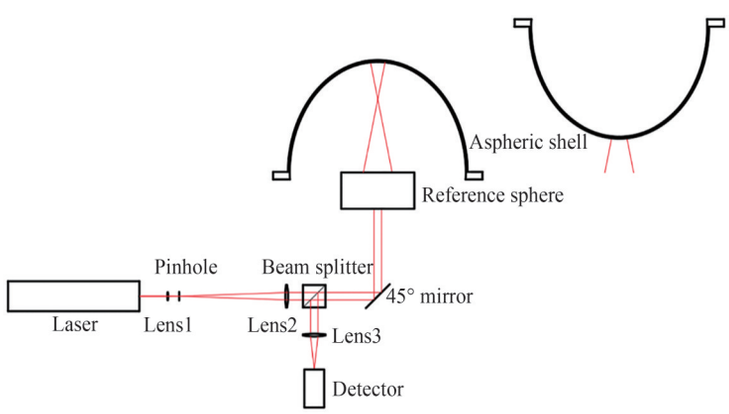

图1 激光干涉仪光路示意

Fig.1 Schematic of the optical path of the laser interferometer

将含有参考球面镜的透镜组安装于回转误差δ_0为0.07 μm的高精度中空气浮转台中[11-12]。调节干涉仪位置使得光轴与转台旋转轴重合，作为参考轴。通过调心调平机构连接被测件和中空气浮转台，当透镜组的焦点位置与非球面被测件最佳拟合球心存在一定的离焦时也可以采集到干涉图。若被测件轮廓旋转轴与参考轴不重合，存在定中偏差，这种定中偏差的存在导致气浮转台旋转的同时条纹整体会随之定点绕圈。通过特征提取算法对被测件不同运动姿态的干涉条纹进行实时处理，得到干涉图整体绕圈半径，定中偏差测量光路示意如图2。

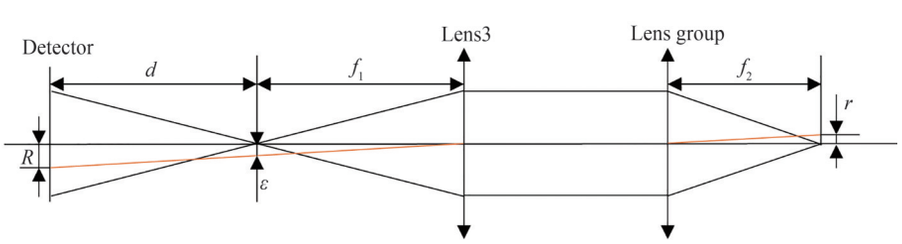

图2 定中偏差测量光路示意

Fig.2 Schematic of the optical path for centering deviation measurement

图中R为干涉图整体绕圈半径，r为定中偏差，f_1、f_2分别为透镜3和透镜组的焦距，d为探测器平面到透镜3焦点的距离，则有[13]

$$r=\frac{f_2\cdot R}{f_1+d} \tag{1}$$

传统的准直定中方法需要进行严格的对焦才能得到定中信号,常用的方法是不断调整被测件的位置,直至目视分划像最清晰,通过分划像的旋转半径来表征定中偏差,但是这只适用于球面定中。本方法不要求被测件球心与汇聚焦点严格重合,不引入离焦误差的同时从原理上使定中信号变得容易发现,从而实现对干涉条纹进行实时分析,且可用于非球面定中测量。

2 定中精度

相较于传统的目视干涉仪通过人眼估计干涉条纹绕圈程度的方法,使用高分辨光电探测技术能够有效提高定中精度,但采用原始干涉条纹得到绕圈半径的方法无法达到亚微米级的定中精度。在此基础上,本文提出了特征提取算法处理干涉条纹,成功提高了定中精度。

2.1 光电探测定中精度

实验采用的探测器像素尺寸为4.8 μm×4.8 μm,相机分辨率为2 592(H)×2 048(V)。一般目视干涉仪定中绝对误差约1/10条纹,在本系统中大约对应6个像素,则其检测绝对误差约28.8 μm。使用CMOS阵列替代人眼,检测误差取决于相机噪声水平。实验中相机的噪声在[a,b]之间服从均匀分布[14],噪声水平为2,则$a=-2$,$b=2$,相机噪声的标准差为

$$S_C=\frac{(b-a)}{\sqrt{12}}=\frac{\left[2-(-2)\right]}{\sqrt{12}}\approx 1.15 \tag{2}$$

探测器的定中精度取决于探测器能探测到的最小强度变化,即旋转前后由于径向错位导致的干涉条纹的强度变化的标准差S_i应大于相机噪声标准差S_C。使用MATLAB对两离焦球面波进行干涉仿真,在距离焦点处d的位置放置观察屏,得到理想干涉图。为了求得最小绕圈半径R_{min},将理想干涉图径向错位R,引起干涉图各个像素的强度变化为I_i,则有

$$S_i=\sqrt{\frac{\sum_{i=1}^{n}\left(I_i-\bar{I}\right)^2}{n-1}}>S_C \qquad R>R_{min} \tag{3}$$

通过仿真得到R_{min}为3个像素,即检测干涉图绕圈半径的绝对误差δ_R为

$$\delta_R=3\times 4.8=14.4\ \mu m \tag{4}$$

此时,错位前后干涉图强度变化量的标准差为$S_i=1.17$。则根据误差传递公式,可由式(1)得到光电探测的激光干涉定中绝对误差δ_r为

$$\delta_r=\frac{f_2\cdot\delta_R}{f_1+d}=5.028\ \mu m \tag{5}$$

2.2 特征提取算法定中精度

由2.1节可知,光电探测的激光干涉定中绝对误差δ_r为5.028 μm,不能满足厚度测量的微米级别精度要求,于是引入特征提取算法,对被测件不同运动姿态的干涉条纹进行动态识别以提高定中精度,程序流程如图3。

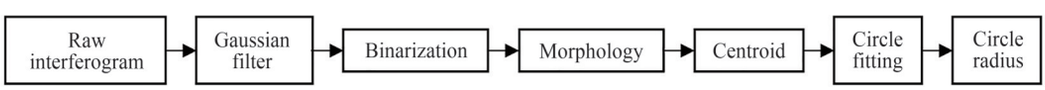

图3 特征提取算法流程

Fig.3 Schematic of feature extraction algorithm flow chart

具体包括对原始干涉图进行滤波,去除背景噪声,接着将图像二值化,使用腐蚀、闭运算、开运算、骨化等图像形态学操作锐化干涉条纹[15],并提取干涉图的质心。使用2.1节获得的理想干涉图进行仿真,结果如图4。使用最小二乘法对一组质心数据进行圆拟合,得到绕圈半径。根据式(1)换算即可分别得到被测件轮廓旋转轴与高精度转台旋转轴之间的误差r。

仿真得到引入特征提取算法后的最小绕圈半径R_{min}为$\frac{1}{4}$个像素,即干涉图绕圈半径的检测绝对误差δ_R为

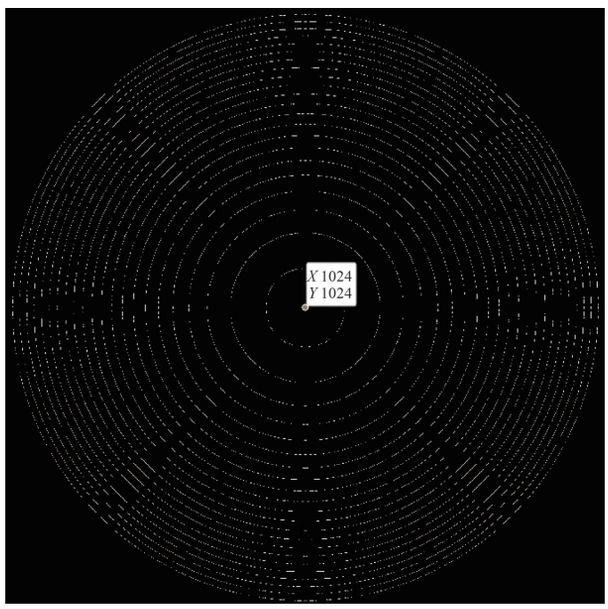

图4 仿真干涉图的图像处理结果示意

Fig.4 Schematic of image processing results of simulated interferogram

$$\delta_{\mathrm{R}}=\frac{1}{4}\times 4.8=1.2\ \mu\mathrm{m} \tag{6}$$

此时,干涉图强度变化量的标准差为

$$S_i=\sqrt{\frac{\sum_{i=1}^{n}\left(I_i-\bar{I}\right)^2}{n-1}}=1.67>S_{\mathrm{C}} \tag{7}$$

则根据误差传递公式,可由式(1)得到最终本系统能检测出的最小定中偏差$r_{\min}$,即定中绝对误差δ_r为

$$\delta_{\mathrm{r}}=\frac{f_2\cdot\delta_{\mathrm{R}}}{f_1+d}=0.419\ \mu\mathrm{m} \tag{8}$$

考虑到高精度中空气浮转台引入的回转误差δ_{O},式(5)修正为

$$\delta_{\mathrm{r}}=\sqrt{\left(\frac{f_2\cdot\delta_{\mathrm{R}}}{f_1+d}\right)^2+{\delta_{\mathrm{O}}}^2}=0.424\ \mu\mathrm{m} \tag{9}$$

对比式(5)和式(9),可知特征提取算法的引入能显著提高本系统的定中精度。

3 实验与结果

为了验证所提方法的定中精度,将全表面PV优于0.4 μm的蓝宝石壳体作为测量对象。为了比对验证,实验中引入了Solartron Metrology公司绝对误差为0.5 μm的电感测微计SI100L对蓝宝石壳体进行测量,如图5所示。蓝宝石壳体随着气浮转台旋转,通过调节调心调平机构减小蓝宝石壳体定中偏差直至电感测微计的示数不再变化,而使用本文方法仍能检测到定中偏差的存在,验证了本文方法定中绝对误差优于0.5 μm,与理论分析结果一致。

在实际测量不透明非球面壳体时,干涉定中装置包括Edmund optics公司型号为1125P的氦氖激光器、去除杂散光的空间滤波系统、若干个调节架、三个透镜、独立设计制造的去球差透镜组、大恒图像公司型号为MER-531-20GM/C-P的探测器、以及用于集成的底板、高精度中空气浮转台和调心调平机构等,如图6所示。根据式(1)可知,要想求出定中偏差,需要得到干涉图绕圈半径。高精度中空气浮转台匀速旋转一周,以等时间间隔实时采集一组干涉图,记录了被测件不同运动姿态的动态特征,再依据2.2节的方法对采集到的干涉图进行实时特征提取算法处理,从而完成定中测量。图7(a)~(d)列出了被测件不同运动姿态下的干涉图测量结果。为了更好地展示不同运动姿态下干涉条纹的变化,在插图中给出了条纹中心部分的放大图,对应的骨化结果也列在插图中。

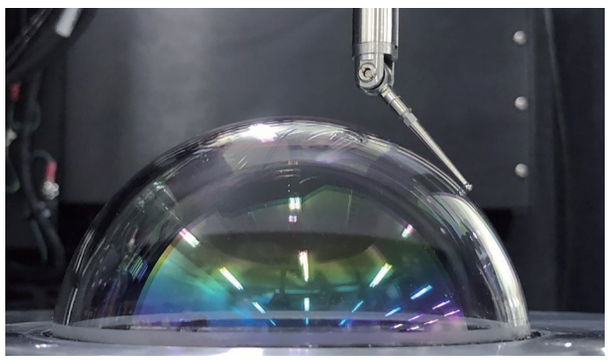

图5　SI100L电感测微计测量示意

Fig.5　Schematic of SI100L inductance micrometer measurement

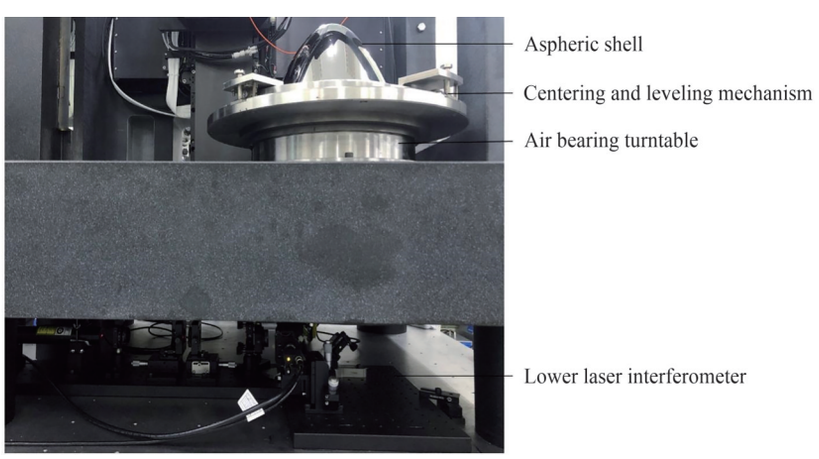

图6　实验装置

Fig.6　Experimental device

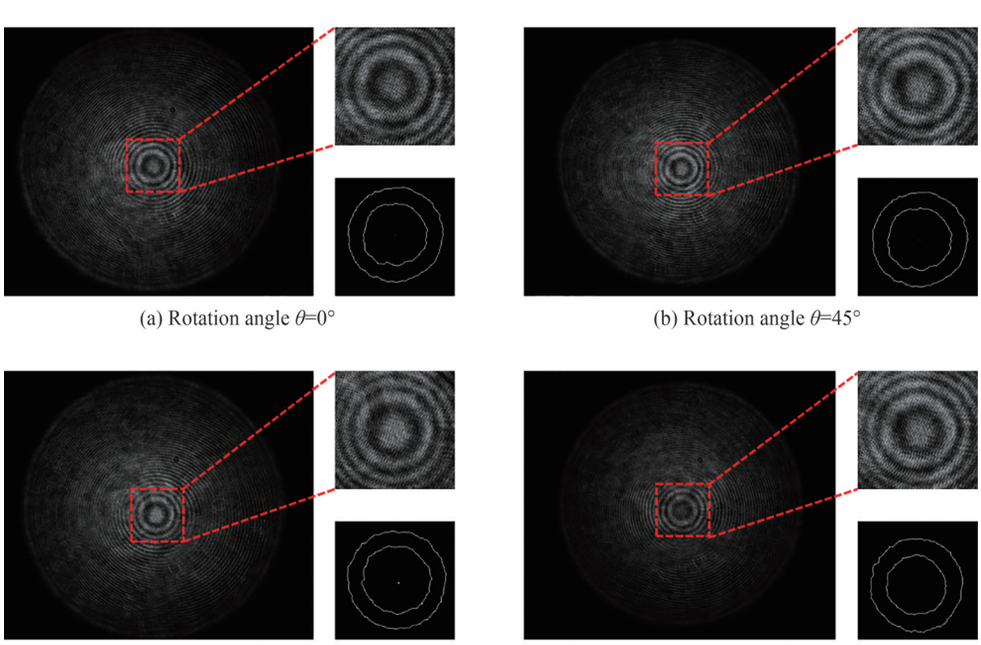

图7　不同运动姿态的实际干涉图及其图像处理结果

Fig.7　Actual interferograms and image processing results with different motion postures

依据2.2节的方法对实际干涉图进行实时特征提取算法处理，得到被测件翻转前后绕圈半径R_1、R_2。代入式(1)可得被测件内、外轮廓旋转轴与转台旋转轴之间的定中偏差r_1、r_2分别为±9.856 μm、±6.202 μm。

综上，对不同运动姿态的被测件进行动态识别，得到翻转前后定中偏差r_1、r_2，即完成不透明非球面壳体翻转测厚过程中基于激光干涉条纹特征提取的定中测量。可为后续利用内外轮廓计算不透明非球面壳体厚度提供数据参考，提高厚度计算准确性。

4 结论

依据不透明非球面壳体翻转测厚过程中严格控制定中精度的需求，本文设计和搭建了双向激光干涉定中装置，引入了现代光电探测技术和特征提取算法，理论推导了该测量系统的定中绝对误差，并进行了实验比对验证，理论分析与实验结果一致，表明所提出的基于激光干涉条纹特征提取的定中方法大幅提高了定中精度，定中测量绝对误差可达0.424 μm。对不透明非球面壳体进行了定中测量，得到翻转前后的定中偏差，为翻转前后被测件内外轮廓旋转轴相对于高精度中空气浮转台旋转轴的偏心提供了数据参考，可用于后续被测件厚度的计算，提高了不透明非球面壳体翻转法测厚的准确性。但在实际应用中发现定中偏差无法达到理想值，经过分析认为是非球面壳体本身轮廓误差对定中精度的影响，未来需要进一步探索更加合适的非旋转量去偶校正算法。

参考文献

[1] CAO Dianye. The measurement and research of residual stresses on the blank of thin-walled parts[D]. Nanjing: Nanjing University of Aeronautics and Astronautics, 2014.
曹殿野. 环形壳体毛坯内应力测量与评估[D]. 南京：南京航空航天大学, 2014.

[2] PANG Lu, ZUO Jianhua, LU Jiping, et al. Analysis of machining deformation of lowt-rigidity parts based on coupled thermal mechanical model[J]. New Technology & New Process, 2015,(1): 43-46.
庞璐, 左建华, 卢继平, 等. 弱刚度零件热力耦合建模及其加工变形分析[J]. 新技术新工艺, 2015,(1): 43-46.

[3] TONG Xin. Research on flexible rotary peen forming for aspherical sheet metal[D]. Xi'an: Xi'an University of Technology, 2019.
童鑫. 金属板件非球面柔性甩打成形研究[D]. 西安：西安理工大学, 2019.

[4] ZHENG Xiaopan. Thin-walled part of variable wall thickness machining modeling and its experimental study[D]. Harbin: Harbin Institute of Technology, 2009.
郑晓盼. 薄壁变壁厚零件切削加工建模及其实验研究[D]. 哈尔滨：哈尔滨工业大学, 2009.

[5] 王伟, 周冠宇, 张祥朝, 等. 一种精准测量薄形零件厚度的装置及方法：中国112113527[P]. 2020-12-22.

[6] HEINISCH J, DUMITRESCU E, KREY S. Novel technique for measurement of centration errors of complex completely mounted multi-element objective lenses[C].SPIE, 2006, 6288:628810.

[7] MA Zhen, LI Yingcai, FAN Xuewu, et al. Study on optical centering of aspheric mirror by interferometry[J]. Acta Photonica Sinica, 2008, 37(7):1455-1458.
马臻, 李英才, 樊学武, 等. 非球面干涉定中方法研究[J]. 光子学报, 2008, 37(7): 1455-1458.

[8] LANGEHANENBERG P, DUMITRESCU E, HEINISCH J, et al. Automated measurement of centering errors and relative surface distances for the optimized assembly of micro-optics[C]. SPIE, 2011, 7926:225-229.

[9] FANG Chao, XIANG Yang. Design of centering system by using collimation and interference with two channels[J]. Acta Photonica Sinica, 2012, 41(10): 1180-1185.
方超, 向阳. 双光路成像干涉定中系统设计[J]. 光子学报, 2012,41(10): 1180-1185.

[10] GROSS H. Handbook of optical systems, volume 1, fundamentals of technical optics[M]. Weinheim: WILEY-VCH Verlag GmbH & Co. KGaA, 2005: 769-772.

[11] XIA Huan, TAO Jizhong, WU Dingzhu. Optimal design of high precision aerostatic swivel table[J]. Machinery Design & Manufacture, 2014(5): 230-232+236.
夏欢, 陶继忠, 吴定柱. 高精度空气静压转台优化设计[J]. 机械设计与制造, 2014(5): 230-232+236.

[12] HUANG Ming, LIU Pinkuan, XIA Yangqiu, et al. Calibration of circular division artifacts using a self-developed angle comparator[J]. Optics and Precision Engineering,2019,27(1):110-120.
黄明, 刘品宽, 夏仰球, 等. 自研角度计量转台在圆分度器件校准中的应用[J]. 光学精密工程, 2019, 27(1): 110-120.

[13] RICHARD D. Contemporary geometric optics[M]. ZHAN Hanqing, transl. Changsha: Hunan University Press, 2004: 44-46.
迪特恩. 现代几何光学[M]. 詹涵青, 译. 长沙：湖南大学出版社, 2004: 44-46.

[14] CAO Hualiang, CHENG Zuhai, YU Liangying. Method to locate accurate center of laser fringe pattern[J]. Computer

Engineering and Applications, 2008,(10):62-63.
曹华梁, 程祖海, 余亮英. 激光干涉条纹中心精确定位方法[J]. 计算机工程与应用, 2008,(10): 62-63.
[15] GENG Shuai, WANG Xichang. An image denoising algorithm based on median filter[J]. Computer and Modernization, 2011,(11): 90-92.
耿帅, 王希常. 一种基于中值滤波的图像去噪算法[J]. 计算机与现代化, 2011,(11): 90-92.

Research on Feature Extraction of Laser Interference Fringe and Centering Measurement Technology

GAO Minge[1], YUAN He[2,3], XU Min[2,3], WANG Junhua[3,4], CUI Hailong[5]
(1 *Academy for Engineering & Technology, Fudan University, Shanghai* 200433, *China*)
(2 *School of Information science and Technology, Fudan University, Shanghai* 200438, *China*)
(3 *Shanghai Ultra-Precision Optical Manufacturing Engineering Center, Shanghai* 200438, *China*)
(4 *Institute of Optoelectronics, Fudan University, Shanghai* 200438, *China*)
(5 *Institute of Machinery Manufacturing Technology, China Academy of Engineering Physics, Mianyang, Sichuan* 621000, *China*)

Abstract: Opaque aspherical shells are widely used in the fields of aerospace, military and communications. The thickness measurement is a key issue to ensure the manufacturing quality of such components. Since it is impossible to conduct micron-level non-destructive measurement of the thickness directly, the flipping measuring method is preferred to measure the inner and outer contours of the shell. The thickness is obtained indirectly through the inner and outer contours. In the flipping measuring method, the centering accuracy before and after the reversal should be guaranteed, which is of significance for specifying the relative positions between the double surfaces. Most of the existing centering measurement technologies are limited by accuracy or complicated structures. Focusing on these limitations, a non-contact centering measurement technology based on laser interference is proposed. The optical structure only consists of two sets of the same laser interference centering device while the measurement accuracy can reach sub-micron level. The specific implementation process is to independently design and set up a bidirectional laser interference centering device and assist the modern photoelectric detection technology and a real-time feature extraction algorithm for laser interference fringes. Finally, the high-precision centering measurement before and after the reversal is achieved. In conjunction with the high-precision hollow air bearing table and a centering and leveling device, a bidirectional laser interference centering device is designed and built to collect the interferograms of the inner and outer surface before and after the reversal. Two sets of the same laser interference centering device are performed up and down to realize the bidirectional centering measurement of the tested part, which can monitor the consistency and tilt of the tested part before and after the reversal. The laser interference centering device adopts the Kepler telescope system to realize the expansion and collimation of the laser beam. The edge stray light is filtered by the pinhole to uniform light intensity. The core of the laser interference centering device is a dedicated lens group containing a reference sphere. This lens group compensates the aberration so that the reference light and the measurement light return back along the same path. The interferograms formed by the reference light and the measurement light are recorded by the detector. Based on the modern photoelectric detection technology, a real-time feature extraction algorithm is proposed to analyze the dynamic characteristics of the interference fringes with different motion postures, which greatly improves the accuracy of dynamic recognition of laser interference fringes. Specifically, the feature extraction algorithm includes filtering, removing background noise, image binarization, image morphology operations such as erosion, closing, opening, and ossification to sharpen the interference fringes, and the centroids extraction of multiple sets of interferograms. The least squares method is used to fit centroids to obtain the least squares radius, which is considered as the radius of rotation of the interferograms. The mathematical model has been built, in which the radius of rotation of the interferogram is treated as the input and the centering deviation of the evolving axis of the opaque aspheric shell and the rotation axis of the hollow air bearing table as the output. Once the radius of rotation of the interferogram is known, the definite centering deviation of the evolving axis of the

opaque aspheric shell and the rotation axis of the hollow air bearing table can be calculated through the mathematical model built. The centering accuracy of the proposed technology is derived theoretically and compared with an inductance micrometer with a certain accuracy in the experiment. The experimental results are consistent with the theoretical results, which proves that the laser interference centering device and real-time feature extraction algorithm can effectively improve the centering accuracy. The absolute centering accuracy can achieve 0.424 microns. The centering measurement is carried out during the thickness measurement of the opaque aspheric shell by the flipping measuring method. Using the laser interference centering device and feature extraction algorithm proposed in this paper, the centering deviations of the evolving axis of the opaque aspheric shell and the rotation axis of the hollow air bearing table before and after the reversal are successfully specified. The centering measurement technology meets the centering requirements and provides a positioning guarantee for the thickness measurement accuracy of the opaque aspheric shell by the flipping measuring method. As a result, the accuracy of profile and thickness measurement of the opaque aspheric shell is improved.

Key words: Interferometry; Feature extraction; Dynamic characteristics; Real-time analysis; Thickness measurement

OCIS Codes: 120.3180; 120.2650; 120.4290

Foundation item: Science Challenge Program (No. JDZZ2016006-01), National Key Research and Development Program of China (No. 2020YFB2007600)